

## Reflection of Very Slow Electrons\*

H. A. FOWLER† AND H. E. FARNSWORTH

*Barus Research Laboratory, Brown University, Providence, Rhode Island*

A monoenergetic electron beam from an electrostatic analyzer has been used to measure reflection coefficients of polycrystalline platinum, single-crystal germanium, and single-crystal copper. The lower limit of primary energy is 0.2–0.3 ev. The contact potential difference between target and collector is measured and compensated by the Kelvin method. Targets are cleaned by heating and argon-ion bombardment. Polycrystalline platinum exhibits a maximum at 2.5 ev, and a rise near zero primary energy attributed to a patch effect. Germanium, after ion-bombardment cleaning, exhibits a low reflection coefficient which decreases to a value between 0.05 and 0.10 at the low-energy limit. Copper, after heating and also after ion-bombardment cleaning, shows a reflection coefficient with weak structure, decreasing nearly to zero at the limit of measurement. These results are in general agreement with the predictions of Herring and Nichols regarding the transparency of surface barriers. Observations have also been made on these targets following argon-ion bombardment and exposure to gases.

### I. INTRODUCTION

THE external reflection of electrons from crystal surfaces in the very low-primary energy range (below 3 ev) has long been a subject of interest in connection with Richardson's equation of thermionic emission. In particular, the value of the external reflection coefficient near zero primary energy is closely related to the surface barrier properties of the crystal. An improved determination of external reflection coefficient has been made in the very low-primary energy range, with particular attention to energy spread of the primary beam, contact potential difference, and surface preparation of the target.

#### 1. Theory

The simplest representations of external reflection assume that the electron is confined to motion in a direction normal to the crystal surface whose potential distribution is represented as one dimensional. Calculations have been made by Schottky,<sup>1</sup> Fowler,<sup>2,3</sup> Nordheim,<sup>4,5</sup> and Eckart<sup>6</sup> on internal reflection coefficients, and by MacColl<sup>7,8</sup> on external reflection coefficients, in this manner. These solutions have been reviewed and interpreted fully by Herring and Nichols<sup>9</sup> who arrive at the general conclusion that a reflection coefficient of the order of 0.05 is to be expected for a clean metal such as tungsten in the very low-energy range.

The possible influence of Bragg reflection on the reflection coefficient has been considered by Kronig

and Penney<sup>10</sup> and by MacColl<sup>8</sup> for one-dimensional models. Morse<sup>11</sup> has considered a semi-infinite three-dimensional crystal. These results and their interpretation have also been discussed by Herring and Nichols. The calculations indicate that Bragg-reflection may contribute to the reflection coefficient at very low-primary energies.

Becker and Brattain<sup>12</sup> and Becker,<sup>13</sup> have neglected the reflection of the electron wave from the surface barrier. They have assumed that externally incident electrons are accelerated at the surface by the inner potential of the crystal and subsequently undergo diffuse scattering. The probability of re-emergence is zero unless the momentum after scattering lies within a "cone of emergence" about the normal to the barrier. Since the apex angle of this cone decreases as the energy of the incident electrons decreases, the fraction of the electrons which escape from the solid approaches zero at the zero of primary energy. This model appears to have been suggested by Schottky's<sup>1</sup> early paper.

#### 2. Previous Experimental Evidence

Support for the specular-reflection model as a valid approximation in the very low-energy range has been given by one of us<sup>14</sup>; for a polycrystalline-iron sample, the reflection becomes progressively more specular as the primary energy is decreased.

Evidence for Bragg reflection was obtained in several experiments by one of us<sup>15–18</sup> before the identification of electron diffraction had been made. Structure is present in the reflection-coefficient curves of polycrystalline targets of Cu, Ni, Fe, W, Ag, Au, Pt, and Pd. The results on several types of copper surfaces have shown definite maxima below 15 ev primary energy for

\* This paper is based on a thesis submitted by H. A. Fowler in partial fulfillment of the requirements for the degree of Doctor of Philosophy in the Department of Physics, Brown University.

† Now at the National Bureau of Standards, Washington 25, D. C.

<sup>1</sup> W. Schottky, *Physik. Z.* **15**, 872 (1914).

<sup>2</sup> R. H. Fowler and L. W. Nordheim, *Proc. Roy. Soc. (London)* **A119**, 173 (1928).

<sup>3</sup> R. H. Fowler, *Proc. Roy. Soc. (London)* **A122**, 36 (1929).

<sup>4</sup> L. W. Nordheim, *Proc. Roy. Soc. (London)* **A121**, 626 (1928).

<sup>5</sup> L. Nordheim, *Z. Physik* **46**, 833 (1928).

<sup>6</sup> C. Eckart, *Phys. Rev.* **35**, 1303 (1930).

<sup>7</sup> L. A. MacColl, *Phys. Rev.* **56**, 699 (1939).

<sup>8</sup> L. A. MacColl, *Bell System Tech. J.* **30**, 888 (1951).

<sup>9</sup> C. Herring and M. H. Nichols, *Revs. Modern Phys.* **21**, 185 (1949).

<sup>10</sup> R. de L. Kronig and W. G. Penney, *Proc. Roy. Soc. (London)* **A130**, 499 (1931).

<sup>11</sup> P. M. Morse, *Phys. Rev.* **35**, 1310 (1930).

<sup>12</sup> J. A. Becker and W. A. Brattain, *Phys. Rev.* **45**, 694 (1934).

<sup>13</sup> J. A. Becker, *Revs. Modern Phys.* **7**, 95 (1935).

<sup>14</sup> H. E. Farnsworth, *Phys. Rev.* **31**, 414 (1928).

<sup>15</sup> H. E. Farnsworth, *Phys. Rev.* **25**, 41 (1925).

<sup>16</sup> H. E. Farnsworth, *Phys. Rev.* **27**, 413 (1926).

<sup>17</sup> H. E. Farnsworth, *Phys. Rev.* **31**, 405 (1928).

<sup>18</sup> H. E. Farnsworth, *Phys. Rev.* **31**, 419 (1928).

many of these surfaces, although one target cut from a single crystal of undetermined orientation has shown almost no structure.<sup>18</sup> A later experiment on the (100) face of a copper-single crystal<sup>19</sup> has permitted concurrent observation of the reflection coefficient and the crystal diffraction pattern. The maxima obtained in the low-energy region are identified with Bragg-reflection beams, as are a large number of slope changes at higher primary energies. In view of these results, the maxima obtained in the earlier results are associated with Bragg reflection from orientated crystallites. Identification of the order of these reflections is greatly complicated by the uncertainty of the experimental inner potential.<sup>19</sup>

Two experiments by Rao<sup>20,21</sup> on polycrystalline and single-crystal nickel have shown similar maxima and changes in slope. These experiments have not permitted concurrent observation of the diffraction pattern. The reflection-coefficient curve obtained from the single-crystal sample has fewer maxima than that from the polycrystalline sample. The interpretation is that diffraction takes place from crystal faces of different orientations on the polycrystalline surfaces.

The first experiment designed specifically to study the very low-primary energy range (below 3 ev) has been that of Farnsworth and Goerke<sup>22</sup> in which a Faraday cylinder has been used as a perfectly-absorbing comparison target. The object here has been to determine the effect on the measured reflection coefficient of the contact potential difference (cpd) between the target and the spherical collector. The results indicate a true reflection coefficient approaching zero as the primary energy is lowered, the limit of measurement being below 1-ev primary energy. The divergence between the true and apparent reflection coefficients observed here has been explained as a result of cpd between the target and collector.

Gimpel and Richardson<sup>23</sup> have criticized this experiment on the grounds that all cpd effects in the target region have not been independently isolated. However, geometrical considerations of the method indicate that any such error in cpd would make the measured value of reflection coefficient too high rather than too low. Their experiment is open to question on the same grounds. Using a polycrystalline-copper target, they have obtained a reflection coefficient which is level at a value of 0.24 from 10-ev down to 4-ev primary energy, passes through a minimum at 2 ev and rises near zero primary energy.

Myers<sup>24</sup> has repeated this experiment, using targets of copper and silver, evaporated on a tungsten sheet.

The outgassed tungsten substrate yields a reflection coefficient with a maximum at 3 ev and a value of 0.12 at the low-energy limit, which is given as 0.5-ev primary energy. Freshly evaporated films of copper and silver show a smooth reflection coefficient with a value of about 0.07–0.08 from 4 ev down to 2 ev, with a slight rise below this primary energy. This rise, like that observed by Gimpel and Richardson, has not been shown unambiguously to be a property of the target surface.

The results of El-Sherbini and Haddara<sup>25</sup> using similar apparatus show maxima in the low-energy region for polycrystalline-copper targets. The accuracy of their measurements in the very low-energy range is doubtful, since the experimental precautions are unspecified.

Hobson<sup>26</sup> has employed an axial magnetic field to collimate the electrons. By this mean Hobson has been able to reach primary energies of a fraction of an ev. His results in the very low-primary energy range, for a copper film evaporated onto a tantalum substrate, show a reflection coefficient approaching zero near the zero of primary energy, in agreement with Farnsworth and Goerke.<sup>22</sup> He has also obtained maxima which are sensitive to the heat treatment of the films. The position of these maxima on the energy scale disagree with those of Farnsworth for the (100) crystal face; this is not surprising, however, in view of the variable structure Hobson has observed.

Recent work by Shelton<sup>27</sup> using an extreme-magnetic collimation technique, indicates a value for the external-reflection coefficient of single-crystal tantalum of about 0.06 at primary energies approaching zero. This particular technique is accurate only at primary energies very close to zero.

## II. EXPERIMENTAL DESIGN AND METHOD

### 1. Difficulties in the Very Low Energy Range

In order to perform an accurate measurement in the very low energy range, special attention must be given to experimental details concerning thermionic energy spread of the primary beam, cpd between the target and the collector, and the surface condition of the target. Without precautions on all of these points, any results below 1-ev primary energy must be considered doubtful. All of the above experiments are subject to criticism on one or more of these grounds.

(a) *Energy spread of primaries.*—Experiments of Boersch<sup>28</sup> and of Hutson<sup>29</sup> have indicated that the width at half-maximum of the thermal-energy spread in electrons from a thermionic source is about 0.8 ev. Such a source is unsatisfactory in the range below 1 ev. Yet nearly all the above experiments have been per-

<sup>18</sup> H. E. Farnsworth, *Phys. Rev.* **34**, 679 (1929).

<sup>19</sup> S. R. Rao, *Proc. Roy. Soc. (London)* **A128**, 57 (1930).

<sup>20</sup> S. R. Rao, *Proc. Roy. Soc. (London)* **A128**, 41 (1930).

<sup>21</sup> H. E. Farnsworth and V. H. Goerke, *Phys. Rev.* **36**, 1190 (1930).

<sup>22</sup> I. Gimpel and O. W. Richardson, *Proc. Roy. Soc. (London)* **A182**, 17 (1943).

<sup>23</sup> H. P. Myers, *Proc. Roy. Soc. (London)* **A215**, 329 (1952).

<sup>25</sup> M. A. El-Sherbini and S. R. Haddara, *Proc. Math. Phys. Soc. Egypt* **3**, 25 (1947).

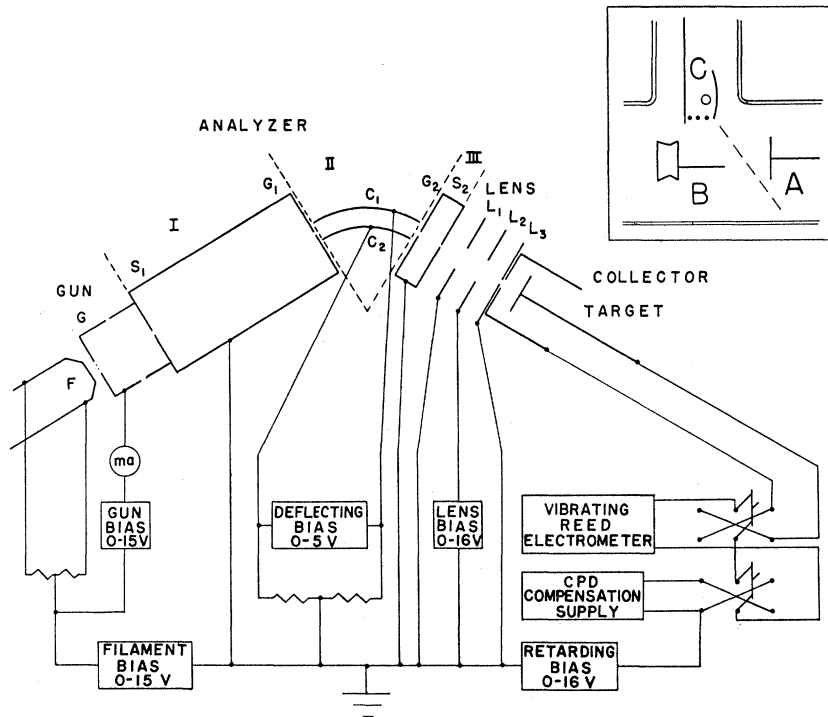
<sup>26</sup> J. P. Hobson, *Can. J. Phys.* **34**, 1089 (1956).

<sup>27</sup> H. Shelton, *Phys. Rev.* **107**, 1553 (1957).

<sup>28</sup> H. Boersch, *Z. Physik* **139**, 115 (1954).

<sup>29</sup> A. R. Hutson, *Phys. Rev.* **98**, 889 (1955).

FIG. 1. Electrode configuration and biasing circuit. *F*: filament; *G*: grid; *S*<sub>1</sub>: entrance diaphragm; *G*<sub>1</sub>: guard diaphragm; *C*<sub>1</sub>, outer deflecting plates; *C*<sub>2</sub>: inner deflecting plate; *G*<sub>2</sub>: guard diaphragm; *S*<sub>2</sub>: exit slit; *L*<sub>1</sub>, *L*<sub>2</sub>, *L*<sub>3</sub>: lens diaphragms. Inset: target and bombardment source; *A*: platinum and germanium target positions during electron and ion bombardments, copper target position during ion bombardment; *B*: copper target position during electron bombardment; *C*: electron and ion source.



formed with unfiltered beams from tungsten filaments, which contain at least this much energy spread. Only the experiments of Farnsworth<sup>14-19</sup> and Farnsworth and Goerke<sup>22</sup> have used oxide-coated filaments, with an energy spread of about 0.4 eV.

(b) *Contact potential difference.*—If the cpd between target and collector, which may be as large as 1.5 v, is not carefully compensated, sufficient electrostatic field may exist between these electrodes to divert the electrons from their intended path. In the preceding experiments, cpd has generally been measured by studying the cutoff of the electron beam when a retarding potential is applied to the target. This method is not independent of either the primary energy spread or the true reflection coefficient of the target, both of which may vary considerably during the life of the experiment. The optimum accuracy of this technique is this technique is probably not better than 0.1 v for the value of the cpd. It is shown in the present paper that a field of 0.1 v between the target and collector introduces errors in the reflection measurement for primary energies below 0.6 eV. The experiment of Farnsworth and Goerke has made evident the importance of an accurate cpd correction.

(c) *Surface condition of target.*—The targets used in the above experiments have been evaporated films, polycrystalline structures, or single crystals. Evaporated films show an uncertain crystal structure and contain many defects unless they are annealed. Polycrystalline structures show a more complicated Bragg-reflection pattern than single crystals. They are also subject to

a patch reflection effect of the type described by Herring and Nichols<sup>9</sup> and Nottingham.<sup>30</sup> Hence, the use of pure, uniform single-crystal surfaces is necessary. Farnsworth,<sup>19</sup> Rao,<sup>21</sup> and Shelton<sup>27</sup> have published the only results for single-crystal targets. The first two experiments were not specifically designed for the very low-energy range.

## 2. Electrostatic Analyzer and Lens System

(a) *Principles.*—The primary-energy spread is reduced by passing the electron beam through an electrostatic analyzer of the cylindrical single-focusing type suggested by Herzog.<sup>31-33</sup> The electrode configuration is shown in Fig. 1. The focusing properties are analogous to those of an optical prism combined with a cylinder lens. Focusing is accomplished by means of three regions of field, separated by the guard diaphragms *G*<sub>1</sub>, *G*<sub>2</sub>. In Region I, which is field free, the electrons diverge from the source aperture *S*<sub>1</sub>. In Region II the beam is deflected by a 64° sector of cylindrical electrostatic field between the deflecting plates *C*<sub>1</sub> and *C*<sub>2</sub>. In Region III, which is also field free, the electrons in a limited energy range (*V*, *V*+ $\Delta V$ ) converge at a common radius in the plane of the exit slit *S*<sub>2</sub>.

The appropriate parameters are chosen in accord with Herzog's analysis (see Table I).

<sup>30</sup> W. Nottingham, in *Handbuch der Physik*, edited by S. Flugge (Springer-Verlag, Berlin, 1956), Vol. 21.

<sup>31</sup> R. Herzog, *Z. Physik* **89**, 447 (1934).

<sup>32</sup> R. Herzog, *Arch. Elektrotech.* **29**, 790 (1935).

<sup>33</sup> R. Herzog, *Z. Physik* **97**, 596 (1935).

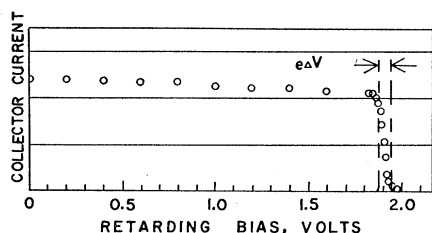


FIG. 2. Curve showing analyzer resolution  $\Delta V/V$ . Arrows indicate limits of expected  $e\Delta V$  for  $\Delta V/V=3\%$ .

The expected  $\Delta V/V$ , considering only the contribution from the width of  $S_1$ , is given by the relation  $\Delta V/V=1/d=1.05\%$ . The finite width of  $S_2$  ( $y_0''=0.008$  cm) adds 1% to this figure. Other contributing factors are momentum spread normal to the plane of deflection, and errors of alignment in assembling the electrodes. These are more difficult to estimate, but a maximum contribution of 1% can be set for each. A reasonable expectation of performance is that all measurable electron current will be concentrated in  $\Delta V/V$  equal to 4%, with most of it within 3%. The spread of primary energy  $e\Delta V$  is determined by the analyzer constant  $\Delta V/V$  and the choice of  $V$  in the analyzer. This  $e\Delta V$  is indicated by a pair of arrows on each curve in Figs. 2-10.

The analyzer is preceded by a cylindrical gun<sup>34,35</sup> designed to produce a maximum collimated beam. The beam emerging from the analyzer slit  $S_2$  is refocused by the electrostatic lens and directed against the target. In passage through the lens, the kinetic energy,  $eV$ , and the energy spread,  $e\Delta V$ , remain unchanged.

(b) *Electrode structure.*—The electrodes are constructed for the most part of sheet chromel, rhodium-

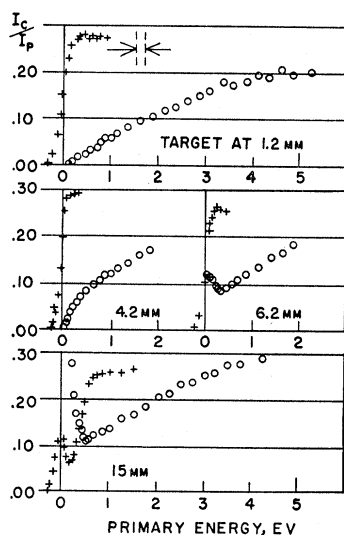


FIG. 3. Curves showing the effect of target position on the measurement of reflection coefficient. The target surface is the same as that for curve 1, Fig. 6.

plated, with circular apertures of the following diameters:  $G=0.3$  cm,  $S_1=0.08$  cm,  $G_1=0.08$  cm,  $G_2=0.08$  cm,  $L_1=0.5$  cm,  $L_2=0.5$  cm,  $L_3=0.1$  cm, collector  $=0.2$  cm.  $S_2$ ,  $L_3$ , and the collector are constructed of platinum foil.  $S_2$  is a slit of width 0.008 cm,  $L_3$  and the collector are separated by spacing of 0.04-0.05 cm.  $C_1$  and  $C_2$  are machined from vacuum-melted copper and plated with rhodium. The construction is made in three subassemblies on a flat molybdenum base plate. Insulation is provided by quartz, glass, and mica spacers, which are kept as far as possible from the path of the electron beam. Shielding and guard electrodes are provided where necessary.

(c) *Biasing scheme.*—The method of biasing the tube is shown in Fig. 1. The choice of filament and deflecting biases determines  $eV$  and  $e\Delta V$  for electrons passing through  $L_3$ . Primary energy at the target is varied by keeping  $V$  constant and applying a retarding bias to the target-collector system. The retarding bias creates a roughly spherical retarding field for the beam, which decelerates it without defocusing. In this manner it is possible to attain primary energies of a small

TABLE I. Parameters of the analyzer.

Deflection angle	$\Phi=\pi/\sqrt{2}$ radius
Mean radius of deflection	$a=a_e=2$ cm
Focal length	$f=\sqrt{2}$ cm
Object distance	$l'=4$ cm
Image distance	$l''=0.5$ cm
Object width (diameter of aperture in $S_1$ )	$y_0'=0.08$ cm
Optical parameter	$x=\sqrt{2}$
Resolving power	$I=a/y_0'[1-\cos(x\Phi) + (l'/a)x \sin(x\Phi)] = 95$

fraction of an ev. A maximum in primary current through  $L_3$  is obtained by adjusting the negative bias on  $L_2$ . This bias should be slightly larger than that on the filament. No bias is applied to  $L_1$ .

(d) *Current yield.*—In the reflection-coefficient measurements to be described, the analyzer has been operated at several values of  $eV$  between 8 ev and 2.5 ev. For  $eV$  lower than 2.5 ev, the current yield has been insufficient for accurate reflection-coefficient measurements. The current yields through  $G_1$  and  $S_2$  for an emission current to grid  $G$  of about 0.6 ma, are shown in Table II.

(e) *Observed spread,  $\Delta V/V$ .*—To provide an experimental confirmation of the analyzer resolution, the target has been removed and the open end of the collector covered with a flat platinum cap. The cutoff in primary current to this closed collector, which functions as a Faraday box, is shown in Fig. 2. Here  $eV$  is equal to 1.90 ev. It will be seen that 70 to 80% of the cutoff occurs within the expected 3% spread. The slope of the low-energy plateau is due to emission-drift, and is not considered significant.

<sup>34</sup> H. E. Farnsworth, J. Opt. Soc. Am. and Rev. Sci. Instr. **15**, 290 (1927).

<sup>35</sup> H. E. Farnsworth, Rev. Sci. Instr. **21**, 102 (1950).

### 3. Target-Collector Assembly

Contact potential difference between the target and the platinum collector has been corrected for by the use of the Kelvin method, which is entirely independent of the reflection coefficient of the target and the energy distribution of the primary beam. The target may be advanced along the beam axis to a position within 0.5 mm of the collector surface, and jerked back a short distance by a magnetic control. The cpd compensation supply, Fig. 1, is then adjusted for null capacitive signal in the collector arm of the circuit. By this method it is possible to measure and compensate cpd to within  $\pm 0.005$  v of instrumental error.

Currents from the target and collector are measured by a vibrating-reed electrometer with input resistances of  $10^9$  and  $10^{10}$  ohms. The electrometer can be transferred by two double-throw switches from the target line to the collector line and back. Since it has a very low effective input impedance, this transfer does not disturb the cpd correction.

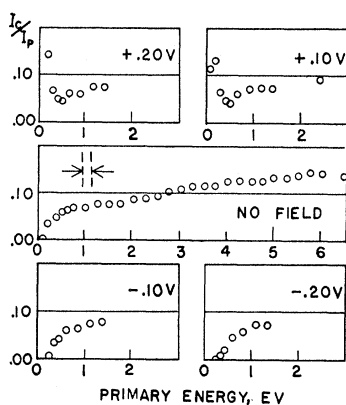


FIG. 4. Curves showing the effect of applied voltage between target and collector. Target surface is the same as that for curve 1B, Fig. 8.

The target is supported by a long molybdenum rod mounted in quartz on a movable carriage. The entire assembly may be retracted magnetically, along a track of tungsten rods, into a side arm of the envelope. Electrical connection is made through a coil spring of fine tungsten wire.

In its retracted position, the target is in the vicinity of the filament-grid assembly *C* shown in the inset in Fig. 1. This may be used either to heat the target by electron bombardment of the back or to clean it by ion bombardment of the front. During electron-bombardment heating, the target is in position *B*, and is maintained 1–3 kv positive with respect to the filament. A 200–250-v positive potential is applied to the grid to furnish the required target current. During ion bombardment the target is in position *A*, and is maintained 600 v negative with respect to the filament. A positive potential of 140–150 v on the grid produces an argon discharge limited to the region shown in front of the target face. An ion current of about 100 microamperes/cm<sup>2</sup> is used.

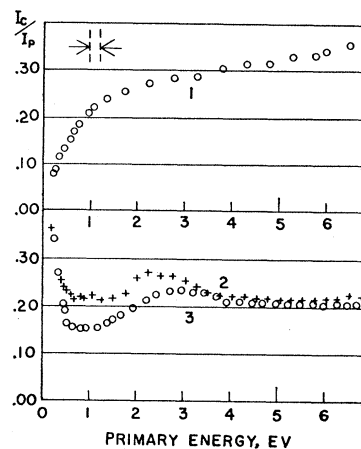


FIG. 5. Reflection coefficient of polycrystalline platinum target I. Curve 1: after tube evacuation and bakeout; curves 2, 3: after argon-ion bombardment and annealing.

As the carriage is retracted into the side arm, a trap door rises between the target and the collector, preventing direct evaporation or sputtering onto the collector surface. The shields shown near the source filament prevent direct evaporation or sputtering from the filament onto the target face.

### 4. Vacuum Conditions and Target Cleaning

The vacuum system is of all-Pyrex construction, and utilizes two single-stage mercury diffusion pumps in series with a liquid-nitrogen trap. Argon is admitted for purposes of ion bombardment, through a capillary-tube leak, a liquid-nitrogen trap, and an evaporated-molybdenum getter tube. Mercury cutoffs outside the traps control the leakage of argon and its exhaust from the experimental tube.

After first evacuation, the tube is ordinarily baked for three hours at 300–350°C, with the traps at dry-ice temperature; it is cooled to room temperature, and the traps are allowed to warm to room temperature for one-half hour; then the dry ice is replaced, and the bakeout is repeated. The main trap is then cooled to liquid-nitrogen temperature two or three times for intervals of an hour, returning to dry ice temperature between

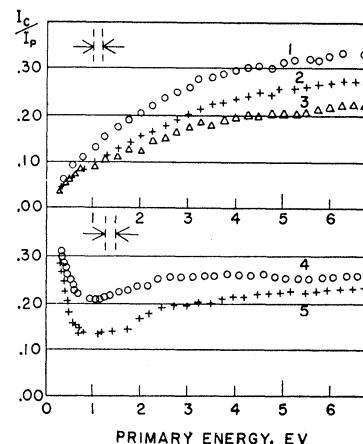


FIG. 6. Reflection coefficient of polycrystalline platinum target II. Curves 1, 2, 3: after argon-ion bombardment, before annealing; curves 4, 5: after exposure to gas.

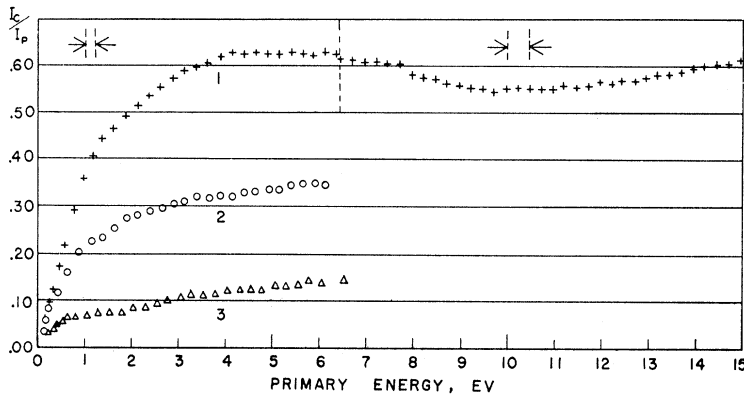


FIG. 7. Reflection coefficient of a single-crystal germanium target, before ion-bombardment cleaning. Curve 1: after etching, tube evacuation, and bakeout; curve 2: after heating one hour at a low temperature; curve 3: after prolonged heating at a high temperature.

these periods. These temperature cycles reduce high-vapor-pressure constituents in the large trap, which is thereafter kept at liquid-nitrogen temperature.

Following this procedure, a pressure of  $5 \times 10^{-9}$  mm Hg is usually read on the ionization gauge, which is of the Bayard-Alpert type. The molybdenum getter is then flashed repeatedly, and after it has been active for several days the residual pressure reading is about 1 or  $2 \times 10^{-9}$  mm Hg. This reading is attained without strenuous heating of the metal parts of the gauge, and represents an upper limit to the total gas pressure within the tube. Under exceptional conditions, when the gauge grid has been well outgassed and the tube allowed to stand with no filaments active for several days, background pressures as  $2 \times 10^{-10}$  mm Hg are read on the ionization gauge.

The pressure of active gas present, particularly oxygen, is considerably lower than the above figure because of the activity of the molybdenum getter.

Targets have been cleaned by the argon-ion sputtering technique developed in this laboratory.<sup>36,37</sup> The targets have been initially outgassed at maximum safe temperatures until an outgassing pressure of  $10^{-7}$  mm Hg or better is obtained. They are then bombarded in the manner described above for 8 to 10 min with an argon pressure of about  $10^{-3}$  mm Hg. The target is then

annealed at a temperature which depends on the material. The cycle of outgassing, ion bombardment, and annealing is repeated until reproducible values of the cpd between target and collector are obtained after the outgassing stage of the cycle. The cpd and reflection coefficient are then observed through each stage of several further cycles. Several important details of the ion-bombardment technique; gettering, trapping, and controlling the discharge, have been discussed elsewhere.<sup>37</sup>

### 5. Procedure for Reflection Measurements

After correcting for the cpd between target and collector to within  $\pm 0.015$  v, the target is placed at a distance of 4.0–4.5 mm from the opening through which the electrons enter the collector. The energy of the primary electron beam passing through the analyzer and lens is adjusted to the highest primary energy desired (usually 2.5 to 10 eV). The energy of the electrons striking the target is decreased in small steps by applying a suitable retarding potential to the target-collector system. Currents to the target and collector are measured by transferring the electrometer with the two double-throw switches.

After plotting the reflection coefficient and the total

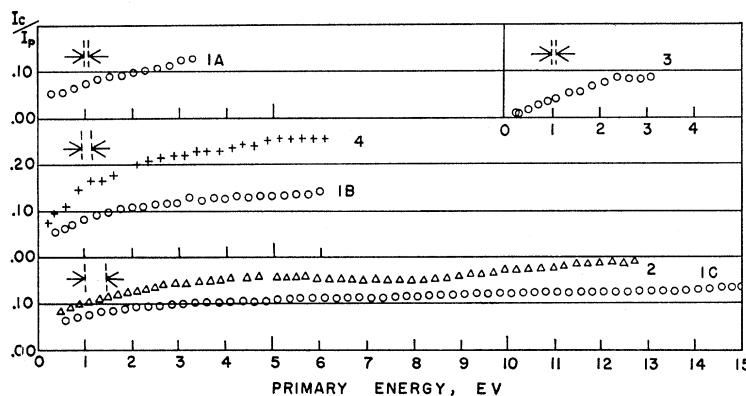


FIG. 8. Reflection coefficient of single-crystal germanium, after ion-bombardment cleaning. Curves 1A, 1B, 1C: after argon-ion bombardment and annealing; curve 2: (100) sample; curve 3: (110) sample after argon-ion bombardment, before annealing; curve 4: after exposure to oxygen.

<sup>36</sup> Farnsworth, Schlier, Burger, and George, *J. Appl. Phys.* **26**, 252 (1955).

<sup>37</sup> J. A. Dillon, Jr., and H. E. Farnsworth, *J. Appl. Phys.* **28**, 174 (1957).

primary current as functions of the retarding potential applied to the target-collector system, the zero of primary energy is determined from the cutoff of the total-current curve, indicated by crosses in Fig. 3. These curves are similar to the one in Fig. 2, but are plotted on a reversed abscissa scale. The zero of primary energy is taken at the point where the total primary current has dropped to one-half its maximum value. Using this zero, the true primary energy is plotted along the abscissa. The minimum before cutoff in the curve for the 15-mm position is caused by electron loss through the opening between the edge of the target and the rim of the collector.

### 6. Precautions and Sources of Error

(a) *Consideration of stray fields.*—The earth's magnetic field has been compensated by Helmholtz coils of radius 30 cm. A high-speed flip coil has been used to measure the residual field in the vicinity of the target. This field has been kept below 0.05 oersted. In such a field, an electron having energy of 0.3 ev has a radius of curvature of more than 40 cm.

TABLE II. Current yields from analyzer.

Energy of transmission (filament bias) volts	Current through $G_1$ amperes	Current through $S_2$ amperes
10	$3 \times 10^{-8}$	$3 \times 10^{-10}$
6	$3 \times 10^{-8}$	$1.5 \times 10^{-10}$
4	$2 \times 10^{-8}$	$4 \times 10^{-11}$
2	$1 \times 10^{-8}$	$1 \times 10^{-11}$
1	$6 \times 10^{-9}$	$? \times 10^{-12}$

Electrostatic effects are those of residual cpd field and retarding potential near the collector entrance. The residual cpd field has been less than 0.015 v. The effect of an electrostatic field between target and collector is shown in Fig. 4. The graphs show the changes produced by varying the voltage in 0.10-v steps. A 0.10-v retarding potential produces an upward break in the curve at about 0.6 ev primary energy, while a 0.10-v accelerating potential causes the reflection coefficient to reach zero at about 0.3 ev. It has been shown that the retarding-potential field does not produce appreciable divergence of the primary beam, by taking observations for various target positions. Figure 3 shows the measured reflection coefficient as a function of primary energy for target positions between 1.2 mm and 15 mm from the beam entrance in the collector. At small values of the above distance, the measured coefficient is too low due to loss of reflected electrons through the entrance aperture in the collector. At large values there is an error due to primary electrons which miss the target. For a target position of 4.0 to 4.5 mm, the sum of these errors is minimized.

(b) *Capacity effects in the measurement of cpd.*—Although the targets vary considerably in their shape,

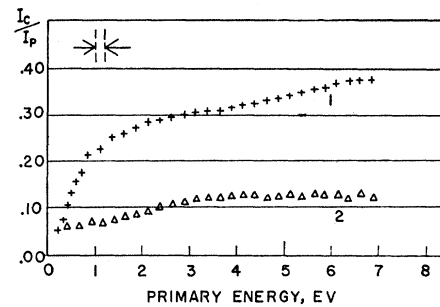


FIG. 9. Reflection coefficient of single-crystal copper, before ion-bombardment cleaning. Curve 1: after etching, tube evacuation, and bakeout; curve 2: after heating to evaporation temperature.

they all have one surface, 8 to 9 mm in diameter, which is parallel to the end of the collecting cylinder. They are supported on the opposite side by a small molybdenum rod perpendicular to the front surface and by a small clamping arrangement. The construction is such that the lateral capacities of the support are small compared to that between the end of the cylinder and the front face of the target when the distance of separation is of the order of 0.5 mm. The rear end of the collecting cylinder is entirely open.

(c) *Instrumental error.*—A small capacitive zero error in the electrometer limits the accuracy of the absolute value of reflection coefficient to  $\pm 0.01$ . In addition, leakage error contributes a small positive slope (approximately 0.03 in the absolute value of  $I_c/I_p$  per 10-ev primary energy) to the curves shown in Figs. 7 and 8. This error varies slightly with the scale of the instrument. A random error in  $I_c/I_p$  of about  $\pm 0.005$  is due to transient electrostatic disturbances caused by switching from target to collector.

Effects of multiple reflection between collector and target appear negligible, since little over-all variation with target position is seen in Fig. 3.

## III. RESULTS AND DISCUSSION

### 1. Polycrystalline Platinum

The platinum target is a disk, 9 mm in diameter and 0.1 mm in thickness, supported by two tabs at its edges

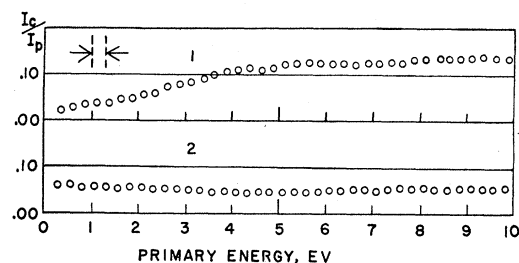


FIG. 10. Reflection coefficient of a (111) copper crystal face, following ion-bombardment cleaning. Curve 1: after annealing 10 min at 700°C; curve 2: after ion bombardment, before annealing.

which are bent back and spot-welded to the molybdenum support rod. This target had undergone extensive outgassing in an earlier vacuum run at temperatures between 1100° and 1200°C. During a brief period of heating at 1300°C to 1400°C recrystallization had occurred, and the target showed a mosaic structure with grain diameter averaging 0.3 mm.

The reflection coefficient after baking out the tube, but before further treatment of the target, is shown in the upper part of Fig. 5. It decreases slowly with decreasing primary energy to about 1 ev, at which point its slope becomes more steep. This type of curve is characteristic of metal surfaces covered with thick layers of gas and impurities. The lower limit of measurement is reached between 0.2 and 0.3 ev; below this point part of the primary energy spread is turned back by the retarding field. The reflection coefficient of this surface is probably similar to that of the platinum collector surface for electrons of normal incidence.

Curves obtained after the annealing phase of two separate target cleaning cycles are shown in the lower part of Fig. 5. The annealing has been carried out at 1100°C for a period of 15 to 30 min or at 700°C for a period of 1 to 2 hours. These two curves are representative of the degree of reproducibility obtained from cycle to cycle.

The maximum observed between 2 and 3 ev corresponds to those for other metals<sup>16,19,21</sup> and is interpreted as a Bragg-reflection effect.

The sharp rise below 1-ev primary energy is attributed to a patch effect from the mosaic structure, of the type discussed by Herring and Nichols<sup>9</sup> and by Nottingham.<sup>30</sup> Patches of high work function repel low-energy electrons, even though the mean cpd between target and collector has been corrected to the full accuracy of the Kelvin method. To test this hypothesis, the target has been made slightly more positive than the potential suggested by the zero of the cpd measurement. A curve corresponding to the "no field" curve of Fig. 4 has been obtained with a cpd overcompensation of approximately 0.4 v. This indicates that the patch effect involves work-function variations of several tenths of an ev over the area of the target surface. The desirability of a single-crystal target is apparent from these results.

The reflection coefficient after ion bombardment, but before annealing, is shown in the top graph of Fig. 6. It is noted that these curves are smoothly decreasing near the zero of primary energy, and attain a very low value at the limit of measurement between 0.03 and 0.05. Clearly the argon layer on the surface smooths out the patch effect and produces an extremely low reflection coefficient in this energy region. When the platinum has been annealed for a few minutes at 700–1100°C, the details in the bottom of Fig. 5 reappear.

The curves labeled 1, 2, and 3 have been obtained in successive ion-bombardment cycles during the early period of activity of the getter. Curve 3 represents the

limiting value attained after the getter has been in operation for about a week; all succeeding curves agreed closely with this one. The reflection coefficient curves at this stage of the cycle all show high stability for periods of several days. If the cleaned and annealed surface is allowed to remain for 15 hours at a residual pressure of  $2 \times 10^{-8}$  mm Hg, curve 4 at the bottom of Fig. 6 is obtained. The same effect has been produced by flashing a fresh filament, to produce temporary pressures above  $10^{-5}$  mm Hg (curve 5). The maximum between 2 and 3 ev primary energy has disappeared because of the adsorption of gas on the surface. However, the rise near zero in primary energy remains, although the upward break comes at a slightly lower value of primary energy, indicating that the patch effect persists through the adsorbed layer in a reduced amount. In each case, the curve characteristic of the clean polycrystalline surface can be recovered by an ion-bombardment cleaning and an hour's heating at 1100°C. The gas-covered surface in these observations is markedly different in character from that of the argon-covered surface following ion bombardment.

In the initial cleaning procedure of the target, comprising several cycles of outgassing at 1100°C and ion bombardment, the work function of the platinum sample rises approximately 0.7 ev and thereafter is reproducible within 0.1 ev after the annealing phase of further cycles. This is in general agreement with the results of Oatley<sup>38</sup> on cleaning a platinum sample. The present sample does not display the large shifts on heating which Oatley attributes to the diffusion of gas from the interior of his sample.

Before the activation of the molybdenum getter, an adsorption effect after heating similar to that described by Harrower<sup>39</sup> has been observed. In the first hour after heating is stopped, the target undergoes a rapid decrease in work function totalling about 0.15 ev. At the same time, a dip in pressure is observed on the ionization gauge. This effect is interpreted as a gettering of the oxygen or carbon monoxide content of the residual gas by the freshly cleaned target surface. The results in the bottom of Fig. 5 were obtained after the getter had been active for a period of several days. No target-gettering effect was observed in connection with these curves. The work function of the target following argon-ion bombardment has shown a scatter of values up to 0.30 ev about the more reproducible value obtained after annealing. Small changes, up to 0.015 ev were often observed in the target work function over the period of a reflection-coefficient run (about forty minutes). However, no changes in target-reflection coefficient were associated with these small changes of work function.

## 2. Single-Crystal Germanium

The sample is cut from a block of 40-ohm-cm, *n*-type germanium in the form of an octagonal disk, 9 mm in

<sup>38</sup> C. W. Oatley, Proc. Phys. Soc. (London) **51**, 318 (1939).

<sup>39</sup> G. A. Harrower, Phys. Rev. **102**, 1288 (1956).



maximum diameter and 2 mm in thickness, with a 3-mm cubic boss projecting from the rear face for mounting purposes. The front face is parallel to a (110) plane of the crystal to within  $0.5^\circ$ .

For the final surface finishing, the face is ground on glass with an emulsion of *M*-305 optical-polishing compound in glycerin and green soap and polished with magnesium oxide and distilled water, on a wax lap. The entire sample is etched with *CP-4F* solution for 30 seconds, and with dilute HF (50%) for one minute. It is then rinsed repeatedly in boiling, doubly-distilled water. This treatment leaves a mirror-like finish which appears, on microscopic inspection, to have a low density of etch pits. Following the etch treatment, the sample is handled only with several thicknesses of filter paper, and care is taken to prevent contamination by dust or moisture.

The target is supported by a light clamp of electropolished molybdenum strip, which is bound to the crystal and to the molybdenum support rod by electropolished molybdenum wire. Thus the only parts of the target support which undergo heating are of electropolished molybdenum.

Four-point probe resistivity tests have been performed on the crystal before and after the vacuum run. The initial value was 40 ohm-cm; the final value, 67 ohm-cm. This is taken to indicate that no bulk contamination of the germanium has occurred during the vacuum treatments.

After the customary bakeout treatment, the reflection coefficient has the unusual high value indicated in curve 1 of Fig. 7. In the very low-primary energy region, this curve drops with a steep slope, approaching zero at zero primary energy, within the limits of error of the measurement. Two observations are shown below 0.3-ev primary energy; although these are questionable, they show a smooth decrease towards the origin. This result, which has been observed also on a crystal cut parallel to the (100) face, appears to be associated with a surface layer left by the etching process.<sup>37</sup> It can be removed by very mild heating. One hour at temperatures of  $350^\circ\text{C}$  to  $400^\circ\text{C}$  reduces it to the value of curve 2. After thirty-six hours of subsequent heating at  $400$ – $475^\circ\text{C}$ , curve 3 is obtained. Following this mild heating it has not been possible to restore the high value of curve 1 by exposure to atmospheric gases, or by baking the tube at  $330^\circ\text{C}$  (at pressures below  $5 \times 10^{-7}$  mm Hg). Each of these processes returns the reflection coefficient to a value near curve 2. The high value of curve 1 has been obtained only after etching the target surface.

The germanium sample from which this target was cut had been previously outgassed for a period of 200 hours between  $600^\circ\text{C}$  and  $700^\circ\text{C}$ , with residual pressures of  $10^{-8}$  mm Hg or less. Extended heating to remove gases from the bulk of the sample has therefore been unnecessary. After 30 hours of heating at  $600$ – $650^\circ\text{C}$  and three or four cycles of ion-bombardment

cleaning, reproducible values of cpd and reflection coefficient have been obtained. After 30 hours of heating and several cycles of ion-bombardment cleaning, the reflection-coefficient curves 1*A*, 1*B*, and 1*C* in Fig. 8 are found to be reproducible and characteristic of the surface. These curves are taken after annealing the surface at  $500^\circ\text{C}$  for one hour. Further heating at temperatures up to  $650^\circ\text{C}$  has no effect on the curves. Curve 1*C* in Fig. 8 shows the range 0–15 ev observed with a broad primary energy spread. Curve 2 shows similar observations on a sample cut parallel to a (100) crystal face, which had undergone pronounced thermal etching during an extended period of heating at  $700$ – $750^\circ\text{C}$ . This sample had also become contaminated with tungsten, but the agreement with the (110) sample is good.

The distinctive features of these curves are that they show no distinct maxima, there is no rise near the zero of primary energy, even in the case of the thermally-etched sample, and they are nearly flat at a value between 0.10 and 0.15 in the range 2 ev to 15 ev. The absence of distinct maxima or any sharp structure in this energy range, appears to be due to the diffraction conditions for these orientations of germanium. The absence of a rise near the zero of primary energy shows that there is no patch effect as in the case of polycrystalline platinum. The low-level value of reflection coefficient at primary energies up to 15 ev cannot be compared with the results of Johnson and McKay<sup>40</sup> which do not extend below 100-ev primary energy.

Curves 1*A* and 1*B* have been obtained from the same surface as 1*C*, using smaller spreads of energy in the primary beam. The curves are considered to be in agreement within the fixed errors of the method of observation. The value of  $I_e/I_p$  at the lower limit of primary energy in curve 1*A* is  $0.07 \pm 0.01$ . Curve 3, Fig. 8, has been obtained after the argon-bombardment phase of the cleaning cycle. The value at the lower limit of primary energy is  $0.02 \pm 0.01$ . Above the range of this graph, the curve is similar to curve 1*C*. This result has been reproduced many times. One hour of annealing at  $500^\circ\text{C}$  is sufficient to remove the argon, and to reproduce curve 1*A*. The rise is reproducible, and lies definitely outside the possible instrumental error.

The effect of exposing the annealed germanium surface to oxygen at pressures of  $10^{-3}$  to  $10^{-4}$  mm Hg for 10 min is shown in curve 4 of Fig. 8. The oxygen used in this test has been admitted through the fore system, and dried by passage through two traps at liquid nitrogen temperature. The measurement has been taken two days after the oxygen exposure. One hour's subsequent heating at  $350$ – $400^\circ\text{C}$  has been sufficient to restore curve 1*B*.

The cpd after annealing has been reproducible over many cycles of cleaning to  $\pm 0.015$  v indicating that outgassing of the sample is relatively complete. In the

<sup>40</sup> J. B. Johnson and K. G. McKay, Phys. Rev. **93**, 668 (1954).

first hour after annealing, the germanium sample generally shows a small decrease ( $<0.020$  v) in work function with time. Following this, it remains stable within 0.005 v for periods up to 48 hours. The work function undergoes a rise of 0.25 v on exposure to oxygen; it returns to its initial value during the short heating described in the last section. These results are consistent with other cpd observations on similar germanium surfaces in this laboratory.<sup>37</sup>

### 3. (111) Face of a Copper Crystal

The copper sample is a prism, 6 mm in length, with a mean diameter of 8 mm. This shape has been chosen because of the tendency of copper to recrystallize during heating. Electron bombardment has been confined to a thin molybdenum sheet covering the back of the sample, and the front face is heated by conduction. Recrystallization has been limited to the immediate vicinity of the molybdenum.

The sample has been ground and polished with its face accurately parallel to the (111) planes of the single crystal. Final polishing has been performed with oiled emery paper, and with *M*-305 lapping compound on a wet wax lap. The entire sample has then been heated in boiling double-distilled water, electropolished for 10 seconds in a 50% solution of phosphoric acid, and rinsed repeatedly in boiling double-distilled water. The result is a highly polished surface with a low density of etch pits. While being mounted, the crystal has come in contact with only clean lens tissue, and has received a last rinse with hot doubly-distilled water just before insertion in the vacuum tube.

The results of simple heating are shown in Fig. 9. Curve 1 shows the reflection coefficient after baking the tube, but before heating the crystal further. Curve 2 shows the value after 10 min of heating at evaporation temperature (800–850°C), with the molybdenum getter active. This curve shows a change of slope at 3.5-ev primary energy, which is probably a diffraction effect of the same general character as the maximum observed for platinum. At the limit of observation, the value of  $I_c/I_p$  is approximately 0.06.

The results after ion-bombardment cleaning are shown in Fig. 10. Reproducible cycles of ion-bombardment cleaning were obtained as soon as the target had been heated to evaporation temperature; this crystal had undergone extensive heating in an earlier experiment. Curve 1 shows the reflection coefficient obtained after 10 minutes of annealing at 700°C (minimum temperature for rapid removal of the argon). A distinct change of slope can be observed in the neighborhood of 4-ev primary energy. The very low-energy region of the curve shows a smooth decrease with decreasing primary energy. The value at the low-energy limit is  $0.02 \pm 0.01$ . Extrapolation would carry the curve through the origin, within the limits of error of the experiment.

Curve 2 shows the reflection coefficient after argon bombardment, but before annealing. This curve has very little in common with the corresponding observations for platinum and for germanium. As is usual for copper samples, the work function of this target rose approximately 1 v during the first heating to evaporation temperature. Thereafter, it has remained reproducible to  $\pm 0.05$  v after the annealing phase of the ion-bombardment cycle. After the argon-bombardment phase, it has assumed a reproducible value  $0.90 \pm 0.05$  v lower than that after the annealing phase. This large reproducible change in the nature of the target surface between the two phases is not attributed to contamination in the argon, because of the precautions described earlier.

All of the curves for the (111) copper show a low reflection coefficient at the low-energy end; there is no indication of an increasing coefficient as the energy approaches zero. The curves for this crystal face show a much smaller amount of structure than those for a (100) face<sup>19</sup> or a polycrystalline surface.<sup>15</sup> However, as noted above, the structure of the reflection-coefficient curve is strongly dependent on the crystal structure and orientation of the reflecting surface; in previous observations by one of us,<sup>18</sup> a copper target cut from a single crystal of undetermined orientation showed almost no structure in the reflection-coefficient curve.

### IV. CONCLUSIONS

The results of this experiment are in general agreement with the prediction of Herring and Nichols,<sup>9</sup> that the external reflection coefficient in the neighborhood of zero primary energy should be 0.05 or less, and are in disagreement with those of Gimpel and Richardson<sup>22</sup> and Myers.<sup>23</sup> This disagreement is most probably the result of patch effects in these two experiments. The results for the two single-crystal surfaces (germanium and copper) after annealing show a very low reflection coefficient in the neighborhood of zero primary energy. All of the curves taken before outgassing or after argon-ion bombardment show a low-reflection coefficient near zero primary energy, although the shape of the curves varies greatly with the target substance and the nature of the covering layer.

The patch effect discussed by Herring and Nichols<sup>9</sup> has been observed for the polycrystalline platinum surface. This effect is not detected in connection with either of the single-crystal targets.

### ACKNOWLEDGMENTS

Assistance by a grant from the Research Corporation of New York is gratefully acknowledged. A Socony-Vacuum Research Fellowship for one year and a Corinna Borden Keen Research Fellowship of Brown University for two years were received by H. A. Fowler.